Why neutrinos oscillate

R. Tegen[a,b*], J.N. Thomas[b,c] and Y. Yan[a]

We discuss recent evidence for the phenomenon of neutrino oscillations, both in vacuum and in matter. This sheds new light on the observed solar neutrino deficit and on preliminary findings of a non-vanishing neutrino mass in recent accelerator-based and underground neutrino experiments.

Introduction

Neutrinos were postulated by Pauli in 1930[1] to explain the β-decay of the free neutron in the reaction[†]

$$n \rightarrow p + e^- + \bar{\nu}_e \qquad (1)$$

without violating the conservation of energy and momentum. Soon afterwards it was realized that this reaction is the fundamental process behind the β-decay of nuclei[‡] according to the reaction ${}^{A}_{Z}X \rightarrow {}^{A}_{Z+1}X' + e^- + \bar{\nu}_e$. Since about 1964, we have known that the fundamental process behind both reactions is the weak decay of the slightly heavier down-quark in the reaction $d \rightarrow u + e^- + \bar{\nu}_e$, via the exchange of a virtual W^- (80419).[2,4,5] The neutrino ν_e is a member of the first of three fermion generations in the Standard Model (SM) (Fig. 1).

$Q/\lvert e\rvert$			
0	$\begin{pmatrix}\nu_e\\ e^-\end{pmatrix}$	$\begin{pmatrix}\nu_\mu\\ \mu^-\end{pmatrix}$	$\begin{pmatrix}\nu_\tau\\ \tau^-\end{pmatrix}$
-1			
$+\frac{2}{3}$	$\begin{pmatrix}u\\ \\ d'\end{pmatrix}$	$\begin{pmatrix}c\\ \\ s'\end{pmatrix}$	$\begin{pmatrix}t\\ \\ b'\end{pmatrix}$
$-\frac{1}{3}$			

Fig. 1. The three fermion generations in the Standard Model: six quarks and six leptons are grouped in three generations. The Glashow-Illiopounos-Maiani (GIM) mechanism prevents the appearance of flavour-changing neutral currents (see text). d',s',b' are mixed (GIM mechanism). ν_e, ν_μ, ν_τ are mixed (ν oscillations).

The first source of neutrinos was identified after the Second World War in the newly-built nuclear reactors with their high flux of neutrons. Reines and Cowan[6] demonstrated in 1953 that indeed (anti)neutrinos are copiously generated during the heat-producing fission process in the nuclear reactor core. Man-made neutrinos had been discovered. Naturally occurring neutrinos were discovered in 1965 by Reines and Sellschop[7] in the deepest mine at that time (near Johannesburg, South Africa) with the then biggest detector.[2,7]

Naturally occurring neutrinos come from two principal sources, the atmosphere, and the Sun. The former are produced by cosmic rays that induce cascades $\pi(K) \rightarrow \mu \rightarrow e$ in the upper atmosphere. Solar neutrinos are by-products of nuclear burning in the Sun (in the p–p chain and CNO cycle, see below). The experimental detection of (anti)neutrinos depends crucially on their expected rest mass. β-decay is a three-body process and as such generates a continuous energy spectrum for the charged lepton in the final state. Initially, only decays involving the electron e^-(0.51)were considered; later the μ^-(105.6) and τ^-(1777) particles were also produced as the so-called final-state leptons in β-decays. Near the end-point energy of the final-state lepton ($E_e^{max} - m_e c^2 = 18.6$ keV for tritium β-decay; $E_e^{max} = 1.29$ MeV for β-decay of the free neutron) linear effects in the neutrino mass are observable, because the anti-/neutrino leaves the interaction region with minimal total energy (almost non-relativistic, see Appendix A and Fig. 2). Quite generally, if one considers the so-called Dalitz plot[§] for a three-body decay $M \rightarrow m_1 + m_2 + m_3$ in the (E_1,E_2) plane (E_2 is the energy of the final-state lepton of rest mass m_2 and E_1 is the corresponding energy of the non-leptonic final-state particle of rest mass m_1), one notices that the upper right-hand corner (where both $E_{1,2}$ are near their maximal values) of the Dalitz plot boundary depends *linearly* on the anti-/neutrino mass (m_3 here). If an experimenter finds no events between the dashed ($m_\nu = 3$ eV) and the continuous boundaries in Fig. 2, this would immediately indicate $m_\nu \geq 3$ eV. Finding events between the dashed and the continuous boundaries would indicate $m_\nu < 3$ eV. This technique has been used continuously to lower the upper bound on the neutrino's rest mass. The upper limit $m_{\bar{\nu}_e} < 500$ eV, set in 1949 by Hanna and Pontecorvo (from tritium β-decay), has come down considerably, to the present $m_{\bar{\nu}_e} < 3$ eV (ref. 3). Other three-body decays have been used over the years to lower the upper limits on m_{ν_μ} and m_{ν_τ}: $\pi^- \rightarrow \mu^- \bar{\nu}_\mu \gamma$ (ref. 8), $\tau^- \rightarrow \pi^- \omega \nu_\tau$ (ref. 9), $\tau^- \rightarrow 5\pi\nu_\tau$ (ref. 3) with the best present limits[3]: $m_{\nu_\mu} < 0.19$ MeV, $m_{\nu_\tau} < 18.2$ MeV.

The present limit for m_{ν_e} of a few eV seems to be a natural barrier for such *kinematical* determinations of the neutrino's rest mass. Although it is highly unlikely that such experiments will lower m_{ν_e} to say, 10^{-3} eV, more surprises cannot be excluded. Recently, two experiments in Mainz[10] and Moscow[11] reached unprecedented levels of sensitivity in determining the number of electrons versus electron energy measured from the β-decay of tritium. Both experiments see a decay anomaly (anomalous peak) between 5 and 15 eV below the maximum β-energy. Close inspection of the energy range 5 eV below 18.6 keV reveals that the location of the peak is well below the point R of the Dalitz plot boundary where the anti-neutrino would be at rest (see Appendix A). While probably not directly related to m_{ν_e}, this unexpected effect has been interpreted as pointing to neutrino relics (a neutrino 'sea' similar to the observed 2.7 K cosmic background radiation photon 'sea').[12]

The above mass limits all refer to Dirac neutrinos, which are distinct from their anti-particles (but have the same Dirac mass).

[a]School of Physics, Suranaree University of Technology, Nakhon Ratchasima 3000, Thailand.
[b]Nuclear and Particle Theory Group, Physics Department, University of the Witwatersrand, Private Bag 3, WITS, 2050 South Africa.
[c]Bard College, P.O. Box 5000, Annandale-on-Hudson, New York 12504-5000, U.S.A.
*Author for correspondence. E-mail: tegen@physnet.wits.ac.za

[†]The reader unfamiliar with the general field of nuclear and elementary particle physics will benefit from first reading the introductory article on neutrinos in this journal (ref. 2). The neutron is heavier than the proton (see rest mass in MeV in brackets throughout the article, data taken from ref. 3). n (939.6) → p (938.3) + e^- (0.51) + $\bar{\nu}_e$ (=0)

[‡]For example (X', X) = (Co, Ni), (B, Be), etc.

[§]The 'Dalitz plot' is named after the theoretical particle physicist R. Dalitz and is defined by the kinematical boundary for the physical events in n-body decay ($n \geq 3$), see Appendix A and Fig. 2. The area within the boundary is usually filled with a great number of dots representing experimental data (so-called events). Any event found outside this boundary would be considered unphysical and would have to be discarded by the experimenter.

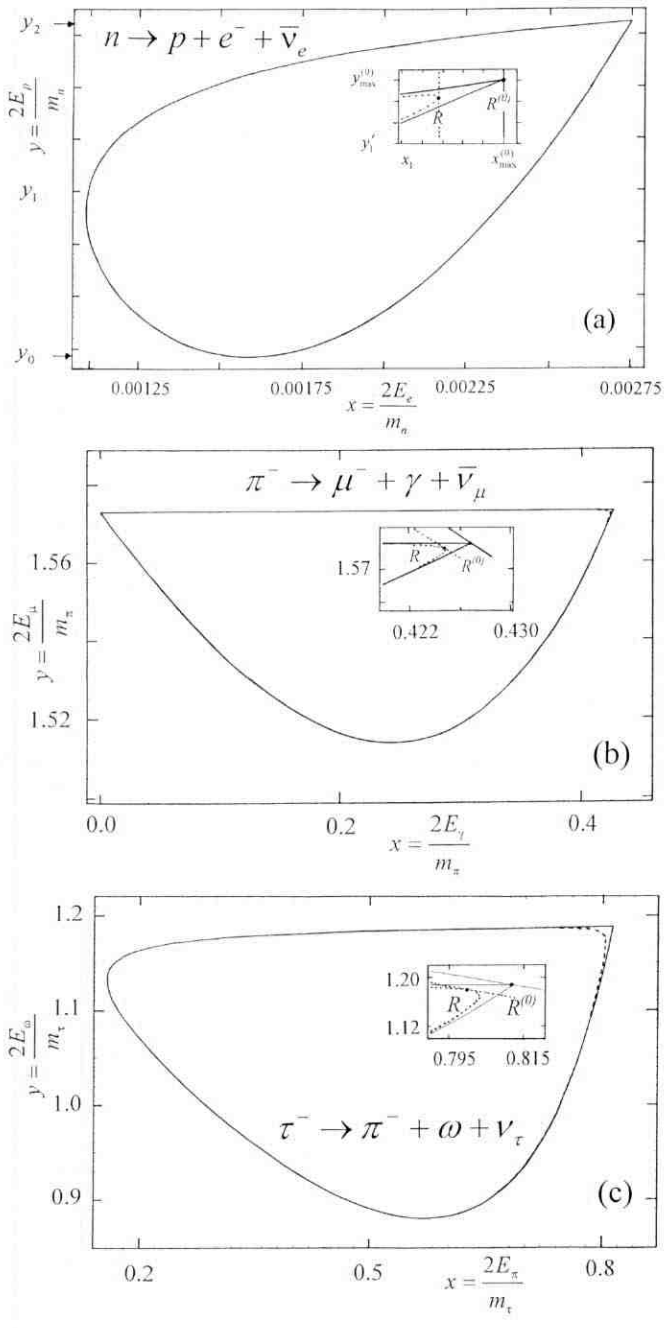

Fig. 2. Dalitz plot boundary for three different β-decays: **a**, $n \to p + e^- + \bar{\nu}_e$, **b**, $\pi^- \to \mu^- + \gamma + \bar{\nu}_\mu$ and (**c**) $\tau^- \to \pi^- + \omega + \bar{\nu}_\tau$. The point R (see text) is the 'intersection' of the upper boundary curve with the straight line $y = 2(1-r_3) - x$; note that the straight line is tangential to the upper boundary curve in R (see Appendix A). In (a) the three points y_0, y_1, y_2 are numerically very close together due to a near-degeneracy of the proton and neutron masses: $y_0 = 1.997246960$, $y_1 = 1.997247760$, $y_0 = 1.997248560$. The point R in (a) is in the upper right-hand corner and is indistinguishable for the two cases '3-eV neutrino' and 'massless neutrino'.

Some electrically neutral particles like photons (γ) and the π^0 (140) are known to be identical to their own anti-particle. Is such a phenomenon restricted to bosons? Neutral fermions comprise neutral leptons (neutrinos) and neutral baryons (neutron, Λ, Σ^0, ...). All neutral baryons are different from their anti-particles. If an (uncharged) neutrino is, however, identical to its own (uncharged) anti-neutrino (a so-called 'Majorana' neutrino, named after the Italian physicist E. Majorana) different experimental techniques have to be used to detect it involving neutrinoless double-beta decay (0νββ), where a neutrino is emitted from one nucleon in a nucleus and re-absorbed as an anti-neutrino by another nucleon in the *same* nucleus, ${}^A_Z X \to {}_{Z+2}{}^A X' + 2e^-$.

Present upper limits are[3,13] $m_{\nu_M} \leq$ several eV, which may be lowered to $m_{\nu_M} \approx 0.04$ eV (ref. 13) with the next generation of 0νββ experiments.

It is apparent that a completely new type of experiment is called for should neutrinos turn out to have rest masses even less than 10^{-2} eV. There is growing evidence that neutrinos have indeed a mass, so *dynamical* neutrino mass effects would be a possible signal to look for.

According to Pontecorvo, tiny neutrino mass *differences* may lead to neutrino oscillations between the three different 'flavours' (Fig. 1), which might be easier to detect than the rest masses themselves, by detecting simultaneously a deficit of one neutrino flavour (say, an electron-neutrino) and an excess of the other neutrino flavours (a muon or tauon neutrino). This oscillation phenomenon per se could explain why we observe fewer electron neutrinos from the Sun than are expected if neutrinos were not to oscillate.

Such experiments fall into two classes: (i) accelerator experiments, and (ii) underground cosmic ray experiments with directional sensitivity.

In the next section, we give the basic principle of vacuum oscillations leading to disappearance and re-appearance probabilities as functions of neutrino energy, distance from source, and neutrino mass information. We then present the basic principle of matter oscillations and show how that could solve the solar neutrino deficit.

The choice of detector depends crucially on the anticipated energy of the anti-/neutrinos. The first generation of chlorine detectors had a threshold of $E_\upsilon = 0.814$ MeV (using the reaction ${}^{37}_{17}\mathrm{Cl} + \nu_e \to {}^{37}_{18}\mathrm{Ar} + e^-$, termed *inverse* β-decay, which excluded most of the neutrinos from the dominant p-p chain, in the Sun). The next generation of gallium detectors is capable of reaching down to 0.233 MeV and will be able to re-examine the solar neutrino deficit. Finally, detectors using the Cerenkov effect in water have a threshold of $E_\upsilon \geq 7$ MeV and will be looking mainly at the blue light cone emitted by high-energy leptons, emerging from the reaction $\nu_l + A \to A' + l$ ($l = \mu^-$ mostly).

The difficulty in identifying ν_τ (as distinct from ν_μ, ν_e) is demonstrated by the fact that it took until the year 2000 before an experiment (the DONUT collaboration at FermiLab[14]) finally verified that $\nu_\tau \neq \nu_{\mu,e}$ by showing that $\nu_\tau + A \to A' + \tau^-$ with no μ^- and e^- in the final state.†

Vacuum oscillations

The idea of neutrino oscillations goes back to Pontecorvo (1957, see ref. 15 for a review). This phenomenon occurs if the mass matrix is not diagonal in lepton flavour space (e^-, μ^-, τ^- neutrino flavours). In that case, the mass eigenstates are different from the flavour eigenstates.

We consider here only two-flavour oscillations by way of illustration,

$$|\nu_e\rangle = \sum_{i=1}^{2} U_{ei} |\nu_i\rangle \qquad (2)$$

with $|\nu_i\rangle$ different mass components (one could be zero or very close to zero), and

$$U = \begin{pmatrix} \cos\theta & \sin\theta\ e^{i\rho} \\ -\sin\theta\ e^{-i\rho} & \cos\theta \end{pmatrix}. \qquad (3)$$

†Note that if oscillation lengths turn out to be $L > 100$ km, the DONUT experiment is not sensitive to neutrino oscillations.

As in ref. 13, we consider a ν_e source at the origin, which emits ν_e particles of total energy E. One assumes $m_i << E$ (for $i = 1, 2$) and easily derives (see Appendix B) the probability of finding ν_e at a distance r from the source (re-appearance mode)

$$P_{\nu_e \to \nu_e}(r) = 1 - \sin^2(2\theta)\sin^2\left(\frac{\pi r}{L}\right), \quad (4)$$

where $L = \dfrac{4\pi E}{|m_1^2 - m_2^2|}$ is the oscillation length.

$P_{\nu_e \to \nu_x}(r) \equiv 1 - P_{\nu_e \to \nu_e}(r)$ describes the 'disappearance mode' (i.e. the probability of finding a muon or tauon neutrino at the expense of an electron neutrino which 'disappeared', i.e. oscillated into something else). A more practical and widely used formula is

$$P_{\nu_e \to \nu_x}(r) = \sin^2(2\theta)\sin^2\left(1.27\frac{\Delta m^2(\mathrm{eV}^2)L(m)}{E(\mathrm{MeV})}\right) \quad (5)$$

with $\Delta m^2 \equiv |m_1^2 - m_2^2|$. The all-important oscillation length L depends on the neutrino energy E and on Δm^2,

$$L = 2.5m\frac{E(\mathrm{MeV})}{\Delta m^2(\mathrm{eV}^2)}. \quad (6)$$

The LSND (Liquid Scintillator Neutrino Detector) group at Los Alamos[16] reported evidence for $\bar{\nu}_e \leftrightarrow \bar{\nu}_\mu$ oscillations and seem to favour $\Delta m^2 \approx 1\ \mathrm{eV}^2$ relatively large, but a small oscillation angle (Fig. 3). LSND detects neutrinos emitted by the LANSCE accelerator with two detectors ≈30 m apart.

According to Equation (6), $L = \dfrac{60m}{2n+1}$ (n = 0, 1,...) should produce the largest $\bar{\nu}_\mu$ deficit for selected neutrino energies $E_\nu \approx$ 24 MeV, 8 MeV, 5 MeV,....

More recently, the Japanese Super-Kamiokande collaboration (ref. 17) reported evidence for $\nu_\mu \leftrightarrow \nu_\tau$ oscillations favouring a maximal mixing angle and much smaller $\Delta m^2 \approx (10^{-3} - 10^{-2})\ \mathrm{eV}^2$. This experiment compares fluxes of neutrinos which have travelled different distances $r_1 \approx 30$ km and $r_2 \approx 12\,000$ km. Here, $L \approx \dfrac{24000}{2n+1}$ km should produce the largest ν_μ deficit, for neutrinos of energy $E_\nu \approx$10 GeV, 3 GeV,... (for $\Delta m^2 \approx 10^{-3}\ \mathrm{eV}^2$ assumed). This simple exercise explains why long-baseline neutrino experiments have been proposed. The K2K Long Baseline Neutrino Oscillation experiment, connecting the Japanese KEK Laboratory and its 'near detector' with the detectors in the Kamioka mine 250 km away, has reported neutrino interactions for the first time. The CERN-Gran Sasso and Fermilab-Soudan projects will involve detectors approximately 800 km apart.

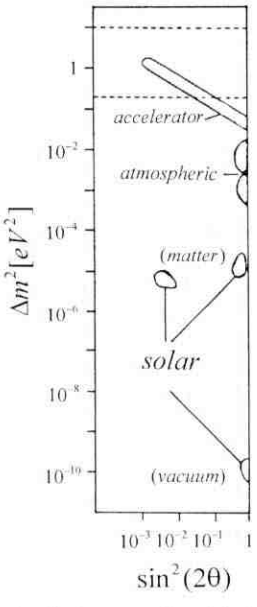

Fig. 3. Schematic view of preliminary experimental evidence for the neutrino mass differences in the double-logarithmic (Δm^2, $\sin^2(2\theta)$) plane. The dashed lines give limits from cosmological, kinematical considerations (non-luminous matter in galaxies), whereas 'accelerator neutrinos' refers to Kamiokande and Super-K experiments, and 'solar neutrinos' refers to the solar neutrino deficit which hints at matter oscillations and vacuum oscillations as indicated (see text).

Matter oscillations

While *vacuum* oscillations might have been seen for the first time only relatively recently, the first evidence for *matter* oscillations goes back nearly forty years, when the solar neutrino deficit was announced by Davies.[17]

The fusion of light nuclei to heavier, more strongly bound nuclei produces the energy radiated from the Sun's surface. The fusion chain begins with hydrogen nuclei which, after several steps, fuse into ^{4}He (this p-p chain reaction is the dominant source of energy for the Sun). For stars heavier than the Sun, the CNO (carbon-nitrogen-oxygen) cycle of nuclear fusion is the dominant source of energy generation. The CNO cycle results in the fusion of four protons into a ^{4}He nucleus ($4\,^1\mathrm{H} \to {}^4\mathrm{He} + 2e^+ + 2\nu_e$ + energy); see ref. 19 for details. The extremely dense shell of the Sun absorbs all of the charged leptons and all nucleons generated in this chain, and only the weakly interacting anti/neutrinos can penetrate the shell. Thus, on Earth we are able to detect the neutrinos that are produced in the fusion chain, but not the other particles. However, the reactions that create the most neutrinos,

$p + p \to {}^2\mathrm{He} + e^+ + \nu_e$ and ${}^7\mathrm{Be} + e^- \to {}^7\mathrm{Li} + \nu_e$

have neutrino energies below 1 MeV and cannot be recorded with chlorine detectors, which, since 1965, record fewer electron-neutrinos than are predicted by the standard solar model.[18,19] All solar neutrino detectors (Super-Kamiokande, SNO, Borexino etc.) have confirmed the Davis result.[18] Detectors using gallium ($E_\nu \geq 0.2$ MeV), chlorine ($E_\nu \geq 0.8$ MeV) and the Cerenkov effect in water ($E_\nu \geq 7$ MeV) measure significantly lower neutrino rates than are calculated by Bahcall for the standard solar model. The deficit in the solar neutrino flux compared with solar model calculations seems to hint at neutrino *matter* oscillations.

The solar neutrino deficit cannot be explained by the vacuum oscillation phenomenon of the previous section. Here the MSW mechanism[20] comes into play. The surprising result is that in matter Δm^2 is much smaller than in a vacuum ($<10^{-5}\ \mathrm{eV}^2$), because the high density of the Sun affects the neutrino flavour eigenstates as they emerge from the core. The Sun is consituted primarily of e^-, p and n (no μ or τ particles), so that the electron neutrino flavour eigenstate $|\nu_e\rangle$ is affected differently from the other neutrino flavour eigenstates $|\nu_{\mu,\tau}\rangle$. This additional phase shift to $|\nu_e\rangle$ changes the quantum mechanical probability of flavour mixing. In order to quantify the effect on a neutrino by a large number of surrounding interacting particles, a refractive index is introduced, by analogy with light travelling through matter.

All neutrino flavours $|\nu_{e,\mu,\tau}\rangle$ interact with matter in the Sun (e^-, n, p) by exchanging Z^0 bosons (a 'neutral current' interaction, see Fig. 4a), while only $|\nu_e\rangle$ participate in the charged current interaction (see Fig. 4b). Mikheyev and Smirnov[20] derived a neutral current refractive index

$$n_{nc} = 1 + 2\pi\rho_e A_{nc}/\vec{p}^2 \quad (7)$$

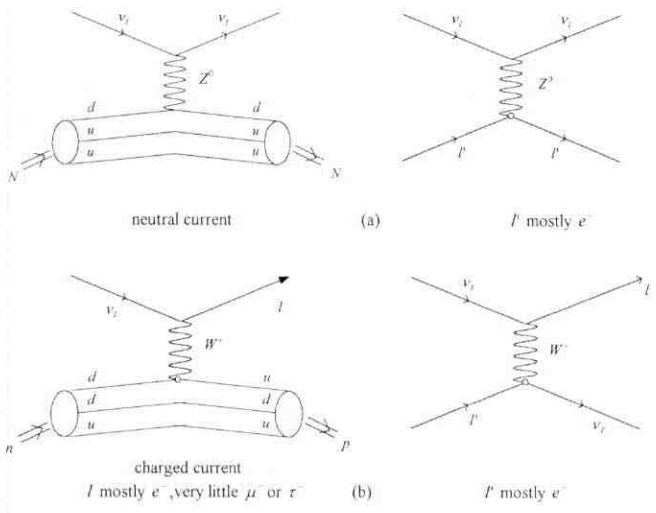

Fig. 4. Feynman diagrams for (**a**) hadronic and leptonic neutral current scattering, (**b**) hadronic and leptonic charged-current scattering processes. In (a) a neutrino elastically scatters off a bound three-quark system (N) or off another lepton l', and exchanges a neutral particle, the Z boson. This process is available to all neutrino species (e, muon or tauon). In (b) a neutrino is converted into its *associated* lepton by exchanging a charged W boson between the nucleon N or lepton l' (see text).

and a charged current refractive index

$$n_{cc} = 2\pi\rho_e A_{cc}/\bar{p}^2, \tag{8}$$

where A_{nc}/A_{cc} is the neutral/charged current forward scattering amplitude, ρ_e is the electron density ($\approx 10^{25}$/cm^3 in the Sun's core) and $|\bar{p}|$ is the neutrino's momentum. The Standard Model gives

$$A_{cc} = \frac{G_F}{\sqrt{2}}\frac{|\bar{p}|}{\pi} \tag{9}$$

and a similar relation for A_{nc}, so that for very high-energy neutrinos, $|\bar{p}| \to \infty$, $n_{nc} \to 1$ and $n_{cc} \to 0$, as expected. The terms $(n_{nc} - 1)$ and n_{cc} are proportional to ρ_e and, hence, vanish in the vacuum.

By analogy with birefringent materials (different refractive indices for independent polarizations of light), the matter in the Sun gives rise to different refractive indices for ν_e compared with $\nu_{\mu,\tau}$. When polarized light travels through a birefringent material, a phase shift arises between the polarization states. Similarly, a phase shift develops between ν_e's and other neutrino flavours after travelling a distance r. Each flavour eigenstate develops a phase $e^{i|\bar{p}|r(n-1)}$, with $n = n_{nc} + n_{cc}$, that is a result of the weak interaction refraction.

The total phase shift experienced by the different neutrino flavours is

$$\delta_e = e^{i|\bar{p}|r(n_{nc}+n_{cc}-1)} = e^{i\rho_e r\left(\frac{2\pi A_{nc}}{|\bar{p}|}+\sqrt{2}G_F\right)} \tag{10}$$

$$\delta_{\mu,\tau} = e^{i|\bar{p}|r(n_{nc}-1)} = e^{i\rho_e 2\pi r\frac{A_{nc}}{|\bar{p}|}}. \tag{11}$$

The extra term $(\sqrt{2}G_F\rho_e)$ present in δ_e is the matter oscillation term. By analogy with the derivation in Appendix B, one obtains

$$P^{MSW}_{\nu_e\to\nu_\mu}(r) = R(\theta)\sin^2\left(\frac{\pi rK}{L_0}\right) \tag{12}$$

with L_0 as in (4),

$$K^2 = \sin^2(2\theta) + (C - \cos(2\theta))^2,\ C = \sqrt{2}G_F\rho_e\frac{2E_\nu}{\Delta m^2},\ R(\theta) = \sin^2(2\theta)/K^2$$

is maximal for $C = \cos(2\theta)$ or, equivalently,

$$\sqrt{2}G_F\rho_e = \frac{2}{L_0}\cos 2\theta, \tag{13}$$

which is known as the matter oscillation resonance equation. Under the condition (13), $R(\theta) \to 1$ and (12) is practically insensitive to the mixing angle θ. Owing to the dependence on ρ_e, a neutrino created in the core of the Sun and travelling outwards will encounter a decreasing ρ_e until, at some distance from the centre, condition (13) is fulfilled.

Following the MSW model, we now take a look at the mass squared matrix for a 2-ν scenario. Standard procedures[20,21] give the eigenvalues as a function of a parameter A (which contains the weak interaction strength and the neutrino energy) and of the mixing angle θ,

$$m_{\nu_l}^2 = \frac{1}{2}(m_1^2 + m_2^2 + A) \pm \frac{1}{2}\sqrt{(\Delta m^2\cos 2\theta - A)^2 + (\Delta m^2)^2\sin^2 2\theta}. \tag{14}$$

Without mixing, i.e. for $\theta = 0$, (14) simplifies to

$$m_{\nu_l}^2 = \frac{1}{2}(m_1^2 + m_2^2 + A) \pm \frac{1}{2}\left|A - \Delta m^2\right|, \tag{15}$$

which gives the two dashed lines crossing at $A = \Delta m^2$ (in Fig. 5). For small A and $\theta = 0$, one expects the muon-neutrino m_2 to be heavier than the electron-neutrino m_1. m_{ν_μ} has then (for $\theta = 0$) no dependence on A, while m_{ν_e} exhibits a linear dependence on A:

$$m_{\nu_e}^2 = m_1^2 + A, \tag{16}$$

which leads to level crossing at $A = \Delta m^2$. For $\theta \neq 0$ no level crossing occurs and one obtains the continuous curves in Fig. 5. For $A >> \Delta m^2$, $m^2_{\nu_e}(A)$ (for decreasing A) will start off on the upper dashed curve and, following the solid curve, will end up on the horizontal dashed curve for small A, hence will emerge as a muon-neutrino with mass $\geq m_1^2$. For $\theta \neq 0$ in (14), one obtains a minimal distance between the two mass squared eigenvalues for

$$A^{(0)} = \Delta m^2\cos 2\theta. \tag{17}$$

From $A \approx \rho_e E_\nu$ one obtains a resonant neutrino energy $E_\nu^{(0)}$ compliant with (17), which is exactly the resonant condition (13) which maximizes (12).

Let us return to the interpretation of Fig. 5. Recall that $A \sim E_\nu$, ρ_e and, hence, the same avoidance of level crossing occurs if $m^2_{\nu_l}$ is plotted versus ρ_e with a closest approach for $E_\nu = E_\nu^{(0)}$. An electron-neutrino created in the Sun's core with energy $E_\nu > E_\nu^{(0)}$ will have to move on the upper continuous curve from right to left until it leaves the Sun's surface as a muon-neutrino. (Note: a neutrino in the core starts with a certain high value of A and, upon travelling to the surface of the Sun, continually lowers the value of A, thereby moving from the right to the left in Fig. 5.). A detector on Earth designed to record electron-neutrinos from the Sun will miss this transmuted neutrino and will signal a solar neutrino deficit. The electron-neutrinos from the Sun that are detected as such must have energies $E_\nu < E_\nu^{(0)}$, otherwise they

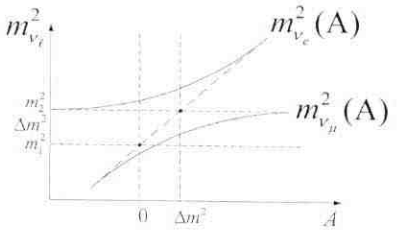

Fig. 5. Δm^2 as a function of A, see Equation (14). The Sun's surface corresponds to the point $A = 0$ (see text).

would appear as muon-neutrinos, if the MSW model is correct.

This implies that $E_\nu^{(0)}$ must be greater than the threshold of the detectors which find a deficit of ν_e's. We conclude that $E_\nu^{(0)} > 5$ MeV. The observation of a high-energy ν_e deficit of ^{8}B neutrinos (with a maximum energy of 14 MeV) gives $E_\nu^{(0)} < 14$ MeV. Thus a rough estimate is

$$5\ \text{MeV} < E_\nu^{(0)} < 14\ \text{MeV}.$$

The resonance condition (13, 17) allows us to estimate Δm^2: If θ is small, (13) reads

$$\Delta m^2 = 2\sqrt{2} E_\nu^{(0)} G_F \rho_e$$

and $\rho_e = 4 \times 10^{25}\,\text{cm}^{-3}$ in the region where the ^{8}B process occurs.[21] Using $G_F = 1.17 \times 10^{-5}\ \text{GeV}^{-2}$ and $E_\nu^{(0)} = 6$ MeV, one gets $\Delta m^2 \approx 6 \times 10^{-5}\ \text{eV}^2$.

Assuming a normal mass hierarchy* for all leptons one obtains for the mass eigenvalues ($m_2 \approx m_{\nu_\mu}$, $m_1 \approx m_{\nu_e}$)

$$m_{\nu_\mu} \approx 8\ \text{meV for } m_{\nu_\mu} >> m_{\nu_e}.$$

Of course the chosen parameters can vary, but it is reasonable to conclude that values for $\Delta m^2 \approx (10^{-4} - 10^{-6})\,\text{eV}^2$, along with a mixing angle given by $\sin^2(2\theta) = 10^{-3}$–$10^{-2}$, allows electron-neutrinos created in the p–p process to persist and those created in the ^{7}Be process to oscillate into muon-neutrinos — thus supporting results from the chlorine, water, and gallium detectors. Another parameter set seems also to be compatible with observations within the rather large uncertainties: $\Delta m^2 \approx (10^{-4} - 10^{-5})\,\text{eV}^2$ and $\sin^2(2\theta)$ close to 1 (Fig. 3). Hence, with the right parameters, the MSW mechanism seems to explain the solar neutrino deficit. A question remains, of course. Is neutrino mixing (if confirmed) unnatural within the Standard Model? It has been pointed out (for example in ref. 21) that a neutrino mass would be easy to implement in the SM without changing its structure.

Consider the three fermion generations in the SM as depicted in Fig. 1. The mixing of (d,s,b) quarks is a natural consequence of the non-observation of flavour-changing neutral currents (named S1 mode); see Fig. 6b for a typical example. The observed (suppressed) S1 mode is due to loop contributions ('penguin' diagram in Fig. 6c). In Fig. 7 we have tentatively drawn analogous diagrams in the mixed neutrino sector. While there are indeed strongly bound neutral mesonic bound states of those mixed (d,s,b) quarks and anti-quarks (see Fig. 6 (a1)) which do not decay (at the dominant tree-diagram level) into $\mu^+\mu^-$ pairs, there are no such $\nu_e\bar{\nu}_x$ ($x = \mu,\tau$) bound states because neutrinos do not participate in the strong interactions. Those diagrams Fig. 7 (a1), (a2) are forbidden by well-tested, charged-lepton family number conservation, $L_\mu \neq L_e \neq L_\tau$. Such exotic $\nu_e\bar{\nu}_x$ ($x = \mu,\tau$) bound states, if they existed as weakly bound states, would have to decay into $\mu^+\mu^-$ pairs via a second-order 'penguin' diagram (Fig. 7). We have calculated that such weakly bound neutrino–anti-neutrino states cannot exist.

*Note that the neutrino mass spectrum could turn out to be degenerate, in which case *direct* neutrino mass determinations as in beta-decay (Fig. 2) would be necessary to determine that one mass m_ν.

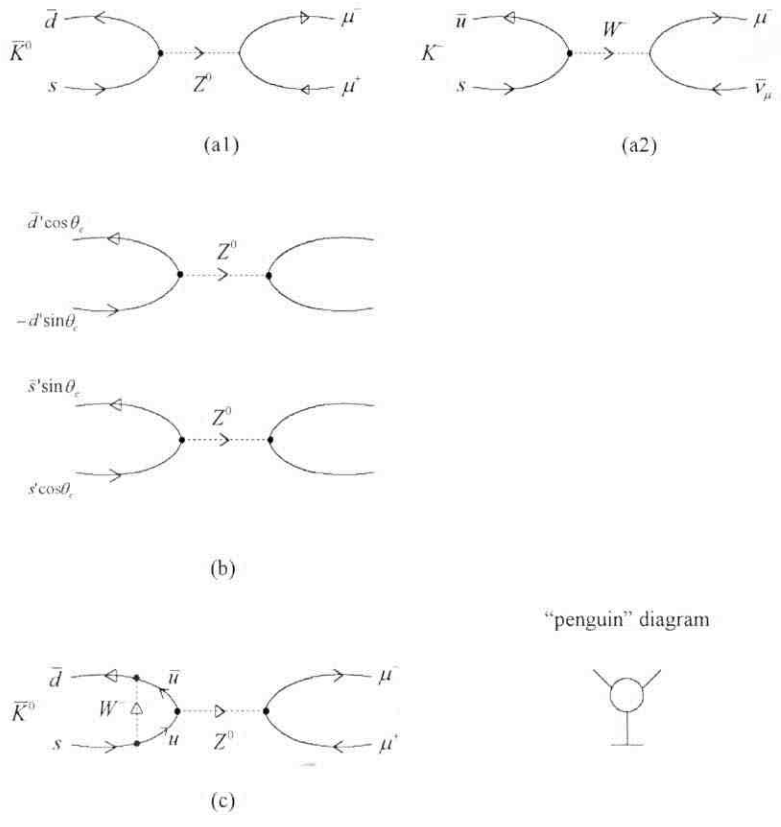

Fig. 6. Feynman diagrams for flavour-changing neutral currents; (**a1**) contribution to $K_L^0 \to \mu^+\mu^-$ without mixing; note the $\bar{d}sZ^0$ coupling is $\frac{G_F}{\sqrt{2}}\cos\theta_c \sin\theta_c$; (**a2**) the corresponding (allowed) charged-current decay of the K^-; (**b**) the GIM mechanism leads to exact cancellation. Now the $\bar{q}qZ^0$ coupling is ($g/\cos\theta_W$), the same for d' and s'; (**c**) second-order effect leads to observed $\approx 10^{-8}$ suppression of this S1 mode.[3] Diagram (**c**) is known as a 'penguin' diagram.

Summary and outlook

Neutrinos and anti-neutrinos are the link or messenger between the Standard Model of elementary particle physics and astrophysics. There is growing evidence that neutrinos have mass and mix, giving rise to oscillation phenomena in both vacuum and matter. Those mixing parameters, once confirmed by independent experiments, will shed new light on both the mass-giving mechanism of the Standard Model and on the interior of stars.

Appendix A. Three-body decay

Let a particle of rest-mass M decay in its rest frame into three particles of rest mass m_1, m_2, m_3. Kinematically allowed pairs of total energies of particles 1 and 2, (E_1,E_2), must lie within the boundaries of the so-called Dalitz plot (Fig. 2). The boundary of the Dalitz plot is given for collinear events. We choose $\vec{k}_1 = -k\vec{n}$; then $\vec{k}_2 = xk\vec{n}$ and $\vec{k}_3 = (1-x)k\vec{n}$ with $0 \le x \le 1$, so that $\vec{k}_1 + \vec{k}_2 + \vec{k}_3 \equiv 0$ for all x. Points of interest on the boundary are $E_1^{\max}, E_2^{\max}$ and the point R for which $E_3 = m_3$ (i.e. particle 3 is at rest). One obtains $E_1^{\max}$ from $k(x)$ maximal, where

$$M = E_1 + E_2 + E_3 = \sqrt{m_1^2 + k^2} + \sqrt{m_2^2 + x^2k^2} + \sqrt{m_3^2 + (1-x)^2k^2} \equiv F(x,k(x)). \qquad (A.1)$$

Hence,

$$O = \frac{dk}{dx} = \frac{-\frac{\partial F}{\partial x}}{\frac{\partial F}{\partial k}} = -kE_1 \frac{xE_3 - (1-x)E_2}{E_2E_3 + x^2E_1E_3 + (1-x)^2E_1E_2},$$

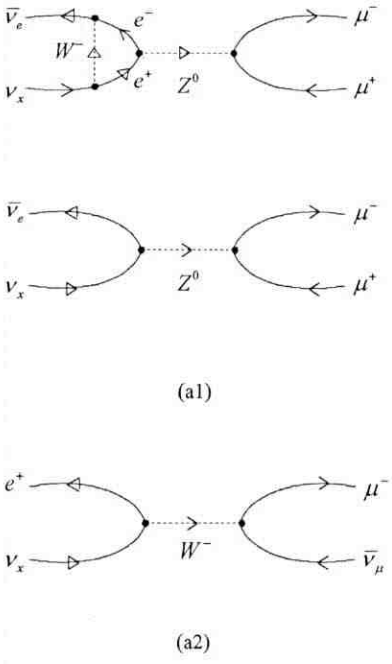

Fig. 7. The top (penguin) diagram is the (supposedly allowed) lepton number-changing neutral decay of a high-energy neutrino. The $We\nu_x$ ($x \neq e$) coupling has, however, not been observed to date. (**a1**) The analogous diagram to Fig. 6 (a1), with $x = \mu$ or τ. (**a2**) The analogous diagram to Fig. 6 (a2), with $x = \mu$ or τ. Both (a1) and (a2) are forbidden by lepton family number conservation.

which gives $x = \dfrac{m_2}{m_2 + m_3}$. We insert x in (1) and obtain

$$E_1^{\max} = \frac{M^2 + m_1^2 - (m_2 + m_3)^2}{2M}. \qquad (A.2)$$

In the same way one obtains

$$E_2^{\max} = \frac{M^2 + m_2^2 - (m_3 + m_1)^2}{2M} \qquad (A.3)$$

and, of course,

$E_{1,2}^{\min} = m_{1,2}$.

Finally, point R is defined by $E_3(R) = m_3$; then

$$E_1(R) = \frac{1}{2(M - m_3)}\left((M - m_3)^2 + m_1^2 - m_2^2\right) \qquad (A.4)$$

$$E_2(R) = \frac{1}{2(M - m_3)}\left((M - m_3)^2 - m_1^2 + m_2^2\right). \qquad (A.5)$$

Now we apply the formulae (1)–(5) to several cases (data are taken from the literature, ref. 3):

(a) $n \rightarrow p + e^- + \bar{\nu}_e$ (see Fig. 1(a))

with $M = m_n = 939.565$ MeV, $m_1 = m_p = 938.272$ MeV, $m_2 = m_e = 0.511$ MeV, and $m_3 = m_{\bar{\nu}_e} = m_{\nu_e}$, we obtain

$$E_e^{\max} = \frac{m_n}{2}\left(1 + \frac{m_e^2}{m_n^2} - \frac{(m_p + m_{\nu_e})^2}{m_n^2}\right) = E_{e,0}^{\max} - m_{\nu_e}\Delta + O\left(\frac{m_{\nu_e}^2}{m_n^2}\right)$$

with $E_{e,0}^{\max} = m_n - m_p + \dfrac{m_e^2}{2m_n} - \dfrac{(m_n - m_p)^2}{2m_n} \approx 1.29$ MeV

and $\Delta \equiv \dfrac{m_p}{m_n} \approx 1 - 10^{-3}$. If the neutrino is at rest the electron energy becomes

$$E_e(R) = \frac{m_n}{2}\left(1 - \frac{m_{\nu_e}}{m_n} - \frac{m_p^2 - m_e^2}{m_n^2\left(1 - \dfrac{m_{\nu_e}}{m_n}\right)}\right) = E_{e,0}^{\max} - m_{\nu_e}\Delta(R) + O\left(\left(\frac{m_{\nu_e}}{m_n}\right)^2\right)$$

with $\Delta(R) = \dfrac{1}{2}\left(1 + \Delta^2 - \dfrac{m_e^2}{m_n^2}\right) \leq \Delta$.

(b) $\pi^- \rightarrow \mu^- + \gamma + \bar{\nu}_\mu$ (see Fig. 2(b))

with $M = m_{\pi^-} = 139.570$ MeV, $m_1 = m_{\mu^-} = 105.658$ MeV $m_2 = m_\gamma = 0$ MeV and $m_3 = m_{\bar{\nu}_\mu} = m_{\nu_\mu}$, we obtain

$$E_\mu^{\max} = \frac{m_\pi^2 + m_\mu^2 - m_{\nu_\mu}^2}{2m_\pi}$$

$$E_{\mu,0}^{\max} = \frac{m_\pi^2 + m_\mu^2}{2m_\pi} = 109.7718 \text{ MeV}$$

$$E_\gamma^{\max} = \frac{m_\pi^2 - (m_\mu + m_{\nu_\mu})^2}{2m_\pi}$$

$$E_{\gamma,0}^{\max} = \frac{m_\pi^2 - m_\mu^2}{2m_\pi} = 29.7982 \text{ MeV}$$

$$E_\mu(R) = \frac{m_\pi}{2}\left(1 - \frac{m_{\nu_\mu}}{m_\pi} + \frac{m_\mu^2}{m_\pi^2\left(1 - \dfrac{m_{\nu_\mu}}{m_\pi}\right)}\right) = E_{\mu,0}^{\max} - m_{\nu_\mu}\frac{1}{2}\frac{m_\pi^2 - m_\mu^2}{m_\pi^2} + O(m_{\nu_\mu}^2)$$

$$E_\gamma(R) = \frac{m_\pi}{2}\left(1 - \frac{m_{\nu_\mu}}{m_\pi} - \frac{m_\mu^2}{m_\pi^2\left(1 - \dfrac{m_{\nu_\mu}}{m_\pi}\right)}\right) = E_{\gamma,0}^{\max} - m_{\nu_\mu}\frac{1}{2}\frac{m_\pi^2 + m_\mu^2}{m_\pi^2} + O(m_{\nu_\mu}^2)$$

$E_\gamma(R)$ is much more sensitive to m_{ν_μ} than $E_\mu(R)$ (see also fig. 3 in ref. 8).

(c) $\tau^- \rightarrow \pi^- + \omega + \bar{\nu}_\tau$ (see Fig. 2(c))

with $M = m_{\tau^-} = 1777.03$ MeV, $m_1 = m_{\pi^-} = 139.57$ MeV

$m_2 = m_\omega = 782.57$ MeV and $m_3 = m_{\nu_\tau} \leq 18.2$ MeV, we obtain (this case is also discussed in ref. 9)

$$E_{\pi,0}^{\max} = \frac{m_\tau^2 + m_\pi^2 - m_\omega^2}{2m_\tau} = 721.68 \text{ MeV}$$

$$E_{\omega,0}^{\max} = \frac{m_\tau^2 - m_\pi^2 + m_\omega^2}{2m_\tau} = 1055.35 \text{ MeV}$$

$$E_\pi(R) = E_{\pi,0}^{\max} - m_{\nu_\tau}\frac{1}{2}\left(1 + \frac{m_\omega^2 - m_\pi^2}{m_\tau^2}\right) + O(m_{\nu_\tau}^2)$$

$$E_\omega(R) = E_{\omega,0}^{\max} - m_{\nu_\tau}\frac{1}{2}\left(1 + \frac{m_\omega^2 - m_\pi^2}{m_\tau^2}\right) + O(m_{\nu_\tau}^2)$$

Appendix B. Neutrino oscillations

If the mass eigenstates are different from the flavour eigenstates (which participate in the expected form in the weak interactions), then each state, say, $|\nu_e\rangle$, contains several mass

components

$$|\nu_e\rangle = \sum_{i=1}^{n} U_{e_i} |\nu_i\rangle \qquad \text{(B.1)}$$

and analogously for $|\nu_\mu\rangle$ and $|\nu_\tau\rangle$. For ease of notation we present here only the 2ν-mixing scheme, i.e. $n = 2$ in (B.1). This scenario includes the LSND $\bar{\nu}_e \leftrightarrow \bar{\nu}_\mu$ and the Super-Kamiokande $\overset{(-)}{\nu}_\mu \leftrightarrow \overset{(-)}{\nu}_\tau$ findings (see main text).

Then

$$U = \begin{pmatrix} \cos\theta & e^{i\varphi}\sin\theta \\ -e^{-i\varphi}\sin\theta & \cos\theta \end{pmatrix}, \qquad \text{(B.2)}$$

where θ is the mixing angle and the phase ρ is disregarded here. (If CP-invariance holds, $e^{i\rho} = 1, i$; the phase ρ is, however, essential for the ovββ scenario[22,23]).

We now assume that a ν_e source at $\bar{x} = 0$ emits ν_e's of energy E, so that

$$|\nu(x)\rangle = e^{-iEt} \sum_i U|_{e_i} \nu\rangle_i \; e^{i\bar{p}_i \cdot \bar{x}},$$

which for $m_i << E$ and $\bar{x} \uparrow\uparrow \bar{p}$ yields ($r \equiv |\bar{x}|$ is the distance from the source and $|\bar{p}_i| \approx E - \frac{m_i^2}{2E}$)

$$|\nu(t,r)\rangle = e^{-iE(t-r)} \sum_i U|_{e_i} \nu\rangle \; e^{-i\frac{m_i^2 r}{2E}}. \qquad \text{(B.3)}$$

The probability amplitude of finding a ν_e at distance r is then

$$\langle \nu_e | \nu(t,r)\rangle = e^{-iE(t-r)} \sum_i U_{e_i} U^*_{e_i} \; e^{-i\frac{m_i^2 r}{2E}}$$

and the 'reappearance' mode (i.e. an initial electron-neutrino remains an electron-neutrino at distance r and time t later) is described by the probability

$$P_{\nu_e \to \nu_e}(r) = \left|\langle \nu_e | \nu(t,r)\rangle\right|^2 = \sum_i \left|U_{e_i}\right|^4 + \sum_{i<j} \left|U_{e_i} U_{e_j}\right|^2 \times 2\cos\left(\frac{2\pi r}{L_{ij}}\right). \qquad \text{(B.4a)}$$

With $L_{ij} = \frac{4\pi E}{|m_i^2 - m_j^2|}$ the oscillation length, (B.4a) simplifies for $n = 2$ considerably to

$$P_{\nu_e \to \nu_e}(r) = 1 - \sin^2(2\theta)\sin^2\left(\frac{\pi r}{L}\right). \qquad \text{(B.4b)}$$

Of course,

$$P_{\nu_e \to \nu_x}(r) \equiv 1 - P_{\nu_e \to \nu_e}(r) \qquad \text{(B.5)}$$

refers then to the 'disappearance' mode (i.e. an electron-neutrino has been transmuted to a muon- or tauon-neutrino). For practical purpose, (B.5) is rewritten in the identical form (5) (see main text).

Received 24 April 2001. Accepted 14 September 2001.

1. Pauli W., letter to a German Physical Society gathering at Tübingen (Germany), on 4 December 1930. Reprinted in *W. Pauli, Collected Scientific Papers*, eds R. Kronig and V. Weisskopf, vol. 2, 1313. Interscience, New York (1964).
2. Johnson C.D. and Tegen R. (1999). The little neutral one: an overview of the neutrino. *S. Afr. J. Sci.* **95**, 13–25.
3. Particle Data Group (2000). Review of particle physics. *Eur. Phys. J.* C15, 1 (for updates visit website: http://pdg.LbL.gov/)
4. Tegen R. (1995). On the mass hierarchy of fundamental particles. *S. Afr. J. Sci.* **91**, 265–270; and (1998). Die topkwark. *S. Afr. Tyd. Natuurw. Tegnol.* **17**, 68–71.
5. Kearns J.P. and Tegen R. (1994). Charge and spin structure of protons, neutrons and pions. *S. Afr. J. Sci.* **90**, 347–353.
6. Reines F. and Cowan C.L. (1959). Free antineutrino absorption cross section, I. Measurement of the free antineutrino absorption cross section by photons. *Phys. Rev.* **113**, 273–279.
7. Reines F. and Sellschop J.P.F. (1965). Evidence for high energy cosmic ray neutrino interactions. *Phys. Rev. Lett.* **15**, 429–433.
8. Missimer J., Scheck F. and Tegen R. (1981). Neutrino masses from three particle decays. *Nucl. Phys.* **B188**, 29–45.
9. Tegen R. (1981). Tau neutrino mass from semileptonic decays. *Z. Phys.* **C11**, 165–168.
10. Weinheimer C. *et al.* (1999). High precision measurement of the tritium spectrum near its endpoint and upper limit on the neutrino mass. *Phys. Lett.* **B460**, 219–226.
11. Lobashev V. *et al.* (1999). Direct search for mass of neutrino and anomaly in the tritium beta-spectrum. *Phys. Lett.* **B460**, 227–235.
12. Gatti F. (1999). Decay anomaly points to neutrino relics. *Physics World* **21**, 21–22.
13. Tegen R. (2000). Do neutrinos have mass? *Proc. Symposium on Fundamental Issues in Elementary Matter*, ed. W. Greiner, pp. 363–370. EP Systema Bt, Publ., Debrecen (Hungary).
14. DONUT Collaboration (2001). Observation of tau neutrino interactions. *Phys. Lett.* **B504**, 218–222. see also http://fnal.gov
15. Pontecorvo B. and Bilenky S.M. (1978). Lepton mixing and the neutrino oscillations. *Phys. Rep.* **41C**, 227–261.
16. The LSND Collaboration (1996). *Phys. Rev. Lett.* **77**, 3082–3085; (1996). *Phys. Rev.* **C54**, 2685–2708.
17. Super-Kamiokande Collaboration. (1998). Study of the atmospheric neutrino flux in the multi-GeV energy range. *Phys. Lett.* **B436**, 33–41.
18. Davis R. (1955). Attempt to detect the anti-neutrinos from a nuclear reactor by the $^{37}_{17}\mathrm{Cl} + \bar{\nu}_e \to {}^{37}_{18}\mathrm{Ar} + e^-$ reaction. *Phys. Rev.* **97**, 766–769. Davis R (1964): Solar neutrinos. II. Experimental. *Phys. Rev. Lett.* **12**, 303–305.
19. Bahcall J.N. (1969). Neutrinos from the Sun. *Sci. Am.* **221**(1), 28–37. Bachall J.N., Calaprice F., Mc Donald A.B. and Totsuka Y. (1996). Solar neutrino experiments: next generation. *Phys. Today* **30**, 30–36.
20. Wolfenstein L. (1978). Neutrino oscillations in matter. *Phys. Rev.* **D17**, 2369–2374. Mikheyev S.P. and Smirnow A. Yu. (1985). Resonance of enhancement of oscillations in matter and solar spectroscopy. *Sov. J. Nucl. Phys.* **42**, 913–917 (translated from *Yad. Fiz.* **42** (1985) 1441–1448).
21. Bahcall J.N. *et al.* (1982). Standard solar models and the uncertainties in predicted capture rates of solar neutrinos. *Rev. Mod. Phys.* **54**, 767–799.
22. Grotz K. and Klapdor H.V. (1989). *Weak Interaction in Nuclear, Particle and Astrophysics*. Teubner, Stuttgart.
23. Wolfenstein C. (1981). CP properties of Majorana neutrinos and double beta decay. *Phys. Lett.* **107B**, 77–79.

NRF series of events on 'Science and Sustainability'

The National Research Foundation is hosting a series of debates, seminars and workshops on science and sustainability, in preparation for the World Summit on Sustainable Development, to be held in Johannesburg from 26 August. Their purpose is to raise national awareness of issues of sustainable development and to involve the research community and civil society.

The current programme of events includes the following:

'The woman in land care and environmental issues in the Limpopo Province', 24 May, Venda Sun (Limpopo). Further information: Karen le Roux (tel. (012) 481-4166; e-mail: karen@nrf.ac.za).

'Recognising, protecting and promoting indigenous knowledge for sustainable development', 7 and 8 June, Kimberley (Northern Cape). Further information: Skamie Mthembu (tel. (012) 481-4069; e-mail: skamie@nrf.ac.za).

'Eradication of poverty', 21 June, Alice (Eastern Cape). Further information: Moiponi Lenyai (tel. (012) 481-4089; e-mail: moipone@nrf.ac.za).

'Pebble bed reactors, nuclear energy and the alternatives', 8 August, Johannesburg Zoo (Gauteng). Further information: Nicoli Koorbanally (tel. (012) 481-4051; e-mail:nicky@nrf.ac.za).

'Working for local environmental efficiency to gain global competitiveness', 13 August, Durban. Further information: Romi Lutchman (tel. (012) 481-4053; e-mail:romil@nrf.ac.za).

'The impact of South African research, education and tourism on one another — using palaeontology, archaeology and geoscience as examples', 21 August, Cape Town. Further information: Michael Nxumalo (tel. (012) 481-4011; e-mail: michael@nrf.ac.za).

Further information on these activities will be carried on the NRF's web site: http://www.nrf.ac.za/jhbsummit